IEEE Access
Multidisciplinary | Rapid Review | Open Access Journal

Received July 31, 2019, accepted August 13, 2019, date of publication August 21, 2019, date of current version September 27, 2019.

Digital Object Identifier 10.1109/ACCESS.2019.2936590

Distributed Robust Adaptive Fault-Tolerant Mechanism for Quadrotor UAV Real-Time Wireless Network Systems With Random Delay and Packet Loss

ZHIFANG WANG, JIANGUO YU, SHANGJING LIN, (Student Member, IEEE), JUNGUO DONG, AND ZHEN YU

School of Electronic Engineering, Beijing University of Posts and Telecommunications, Beijing 100876, China

Corresponding author: Zhifang Wang (zhifang920124@bupt.edu.cn)

This work was supported in part by the National Natural Science Foundation of China under Grant 61531007 and Grant 61701034, and in part by the China Postdoctoral Science Foundation under Grant 2017M620696.

ABSTRACT This research combines a next-generation wireless network and a quadrotor unmanned aerial vehicle (UAV) to create a real-time wireless network quadrotor UAV flight control system. Three major problems will occur when the system operates, such as external disturbances, internal actuator failures and wireless network association failures (random delay and packet loss). We propose a hierarchical distributed comprehensive robust adaptive fault-tolerant control algorithm based on robust fault-tolerant theory to improve the performance of this system. The simulation and flight experimental test results show that when this system is analyzed with respect to external disturbances, internal actuator failures and wireless network association failures, the designed controller stability is asymptotically stable, the performance of this system is very good and the system provides a strategy for establishing a ground-to-air self-organizing wireless network.

INDEX TERMS Quadrotor UAV, real-time wireless network system, distributed robust adaptive fault-tolerant mechanism.

I. INTRODUCTION

With the development of cross-integration disciplines such as control theory and control engineering, communication systems, automation technology, and wireless communication, today's control systems are becoming increasingly complicated. The properties of control objects are becoming less restricted by the disciplines, and the performance standards of control systems are also increasing. The real-time wireless network quadrotor unmanned aerial vehicle (UAV) flight control system is an integrated modern communication system, with control algorithms and a remote flight control system. The system incorporates the characteristics of wireless communication networks and control technologies, includes the advancement of computer and wireless communication network technology into the control field and also reflects the integrated development trend of automatic control systems in networks, integration and layered distribution. Therefore, studying a wireless networked quadrotor flight control system has considerable research value and applications.

The associate editor coordinating the review of this article and approving it for publication was Hamed Ahmadi.

II. MATHEMATICAL MODEL OF A QUADROTOR UAV

From references [1]–[3], we can obtain a mathematical model of a quadrotor, and the transfer functions of the three angles of pitch angle, roll angle and travel angle are as follows:

The dynamic model of a quadrotor UAV is given by equation (1):

$$\begin{cases} \dot{\boldsymbol{L}} = v \\ m\ddot{\boldsymbol{L}} = \boldsymbol{F}_u - mg \\ \dot{\boldsymbol{R}} = \boldsymbol{R}\boldsymbol{S}(\lambda) \\ \boldsymbol{I}\dot{\boldsymbol{\lambda}} = -\boldsymbol{\lambda} \times \boldsymbol{I}\boldsymbol{\lambda} + \boldsymbol{F}_u \end{cases} \tag{1}$$

The mathematical model of the quadrotor UAV is given by equation (2):

$$\begin{cases} I_{xx}\ddot{\phi} = \dot{\theta}\dot{\psi}\left(I_{yy} - I_{zz}\right) + lU_2 \\ I_{yy}\ddot{\theta} = \dot{\phi}\dot{\psi}\left(I_{xx} - I_{zz}\right) + lU_3 \\ I_{zz}\ddot{\psi} = \dot{\theta}\dot{\phi}\left(I_{xx} - I_{yy}\right) + U_4 \\ \begin{bmatrix} m\ddot{x} \\ m\ddot{y} \\ m\ddot{z} + mg \end{bmatrix} = \begin{bmatrix} \cos\phi\cos\psi\sin\theta + \sin\phi\sin\psi \\ \cos\phi\sin\theta\sin\psi - \sin\phi\cos\psi \\ \cos\phi\cos\theta \end{bmatrix} \\ \sum_{i=1}^{4} K_p\omega_i^2 \end{cases} \tag{2}$$

The transfer function of the pitch angle channel is given by equation (3):

$$\boldsymbol{G}_1(s) = \frac{\theta}{\boldsymbol{U}_1} = \frac{56.951s + 4391.1}{s^3 + 105s^2 + 870s + 4430} \tag{3}$$

The transfer function of the travel angle channel is given by equation (4):

$$\boldsymbol{G}_2(s) = \frac{\phi}{\boldsymbol{U}_2} = \frac{65s + 4560.1}{s^3 + 109s^2 + 1023s + 2935.1} \tag{4}$$

The transfer function of the roll angle channel is given by equation (5):

$$\boldsymbol{G}_3(s) = \frac{\theta}{\boldsymbol{U}_3} = \frac{105}{s^2 + 413s} \tag{5}$$

The meanings of the various parameters in the above formulas are specifically referenced in [1]–[3].

III. MATHEMATICAL MODEL OF a SYSTEM FAULT

Establishing an integrated model that includes UAV actuator failures and wireless network association failures, we can use $g_{if}^{hF}(t)$ to indicate that the ith actuator has failed [4], [5] and use $v_{if}^{hF}(t)$ to indicate that the ith wireless associated link channel has failed. The comprehensive fault model is defined in equation (6) as follows:

$$\begin{cases} \boldsymbol{g}_{if}^{hF}(t) = \left[\boldsymbol{I} - \boldsymbol{\rho}_{if}^{h}(t)\right]\boldsymbol{g}_i(t) + \boldsymbol{\Delta}_i\boldsymbol{\varepsilon}_i(t), \\ \qquad\qquad 0 < \rho_{if}^{h} \le \rho_{if}^{h} \le \bar{\rho}_{if}^{h} \\ \boldsymbol{v}_{if}^{hF}(t) = \sigma_{ji}^{h}v_{ij}(t), \quad 0 \le \sigma_{ji}^{h} \le \sigma_{ji}^{h} \le \bar{\sigma}_{ji}^{h} \end{cases} \tag{6}$$

In equation (6), we use $g_i(t)$ to represent the failure type of the quadrotor UAV actuator, $\boldsymbol{\Delta}_i$ to represent the unknown constant, $\boldsymbol{\varepsilon}_i(t)$ to represent the external disturbance, ρ_{if}^{h} to represent the failure factor of the quadrotor UAV actuator, $\underline{\rho}_{if}^{h}$ to represent the lower bound of the failure factor, $\bar{\rho}_{if}^{h}$ to represent the upper bound of the failure factor [6], [7], σ_{ji}^{h} to represent the failure factor of the failure of the wireless associated link channel, $\underline{\sigma}_{ji}^{h}$ to represent the lower bound of the failure factor, and $\bar{\sigma}_{ji}^{h}$ to represent the upper bound of the failure factor; $i, j = 1, 2\ldots, N$, $f = 1, 2, \ldots, m_i$, $h = 1, 2, \ldots, L$, h indicates the h-th failure mode that has occurred and L represents the total number of failure modes. Now, make the following rule:

When $\underline{\rho}_{if}^{h} = \bar{\rho}_{if}^{h} = I = \underline{\sigma}_{ji}^{h} = \bar{\sigma}_{ji}^{h}$, the whole system's function is operating normally; when $\underline{\rho}_{if}^{h} = \bar{\rho}_{if}^{h} = 0 = \underline{\sigma}_{ji}^{h} = \bar{\sigma}_{ji}^{h}$, there is an interrupt fault that occurs in the system; when $0 \le \underline{\rho}_{if}^{h} \le \bar{\rho}_{if}^{h} \le I$, $0 \le \underline{\sigma}_{ji}^{h} \le \bar{\sigma}_{ji}^{h} \le I$, the whole system has partial failed faults [8], [9].

Next, we can provide a comprehensive definition for the system fault in equation (7) as follows:

$$\begin{cases} g_{if}^{hF}(t) = \left[g_{if1}^{hF}(t), \ldots, g_{ifm_i}^{hF}(t)\right]^T = \rho_i^h u_i(t) \\ v_{ij}^{hF}(t) = \left[v_{ij1}^{hF}(t), \ldots, v_{ijq_{ji}}^{hF}(t)\right]^T = \sigma_{ji}^{h}v_{ij}(t) \end{cases} \tag{7}$$

In equation (7), we define 2 parameters: ρ_i^h and σ_{ji}^{h}. Equation (8) is as follows:

$$\begin{cases} \rho_i^h = diag\left[\rho_{if1}^h, \ldots, \rho_{ifm_i}^h\right], \quad \rho_{if}^h \in \left[\underline{\rho}_{if}^h, \bar{\rho}_{if}^h\right] \\ \sigma_{ji}^h = diag\left[\sigma_{ji1}^h, \ldots, \sigma_{jiq_{ij}}^h\right], \quad \sigma_{jik}^h \in \left[\underline{\sigma}_{jik}^h, \bar{\sigma}_{jik}^h\right] \end{cases} \tag{8}$$

For convenience of description, the entire failure mode encountered by the system is abbreviated by equation (9) as follows:

$$\begin{cases} g_{if}^{hF}(t) = \rho_i^h u_i(t), \quad \rho_i^h \in \left\{\rho_i^{h1}, \ldots, \rho_i^{hL}\right\} \\ v_{ij}^{hF}(t) = \sigma_{ji}^h v_{ij}(t), \quad \sigma_{ji}^h \in \left\{\sigma_{ji}^{h1}, \ldots, \sigma_{ji}^{hL}\right\} \end{cases} \tag{9}$$

The comprehensive system equation for the real-time wireless network associated link under the quadrotor UAV is given by equation (10):

$$\begin{bmatrix} \dot{x}_i(t) \\ y_i(t) \end{bmatrix} = \begin{bmatrix} \boldsymbol{A}_{1T}^i & \boldsymbol{A}_{1S}^i & \boldsymbol{B}_{1d}^i & \boldsymbol{B}_{1u}^i \\ \boldsymbol{A}_{2T}^i & \boldsymbol{A}_{2S}^i & \boldsymbol{B}_{2d}^i & \boldsymbol{B}_{2u}^i \end{bmatrix} \begin{bmatrix} x_i(t) \\ v_i(t) \\ \varepsilon_i \\ u_i(t) \end{bmatrix} \tag{10}$$

Then, we have

$$\dot{x}_i(t) = \boldsymbol{A}_{1T}^i x_i(t) + \sum_{j=1}^{N} \boldsymbol{A}_{1S}^{ij}\sigma_{ji}^h\boldsymbol{A}_{2T}^{ji}x_j(t) + \boldsymbol{B}_{1u}^i\rho_i^h u_i(t) + \boldsymbol{B}_{1d}^i\varepsilon_i \tag{11}$$

IV. DESIGN OF THE DISTRIBUTED ROBUST ADAPTIVE FAULT-TOLERANT CONTROLLER

The overall system flow control diagram is shown in Figure 1.

The distributed robust adaptive fault-tolerant controller is designed according to equation (12):

$$u_i(t) = \hat{K}_1 x_i(t) + \sum_{j=1}^{N} \hat{K}_2\sigma_{ji}^h(t)\hat{K}_3 x_j(t) + \hat{K}_4\varepsilon_i(t) \tag{12}$$

K_1, K_2, K_3, K_4 are matrices with appropriate dimensions, and $\hat{K}_1$, $\hat{K}_2$, $\hat{K}_3$, $\hat{K}_4$ are the corresponding estimate values.

The closed-loop control system is given by equation (13):

$$\begin{aligned} x_i(t) = &\left[\boldsymbol{A}_{1T}^i + \boldsymbol{B}_{1u}^i\rho_i^h\hat{K}_1(t)\right]x_i \\ &+ \sum_{j=1}^{N}\left[\boldsymbol{A}_{1S}^{ij}\sigma_{ji}^h\boldsymbol{A}_{2T}^{ji} + \boldsymbol{B}_{1u}\rho_i^h K_2\hat{\sigma}_{ji}^h(t)\hat{K}_3(t)x_j(t)\right] \\ &+ \boldsymbol{B}_{1u}^i\hat{K}_4\hat{\sigma}_{ji}^h\varepsilon_i(t) + B_{1d}^i\varepsilon_i \end{aligned} \tag{13}$$

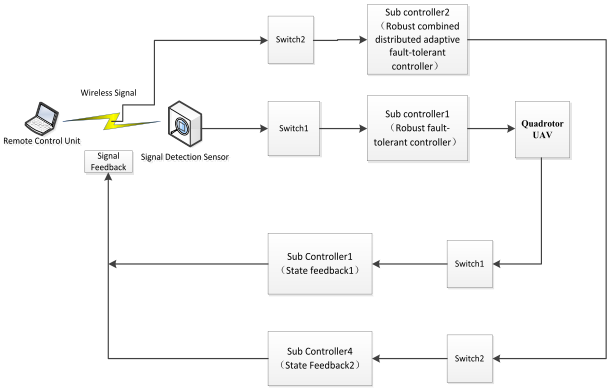

FIGURE 1. System structure.

To prove that the system is asymptotically stable, we first we introduce the following definitions :

$M_i = x_i^T P_i B_{1u}^i$, $R_i = \sum_{j=1}^{N} K_2 \hat{\sigma}_{ji}^h \hat{K}_3 x_j$, $S_i = \hat{K}_4 \varepsilon_i$, where $i = 1, 2, \ldots, N$, P_i is a positive definite symmetric matrix, and M_i, R_i, S_i are bounded vectors expressed as follows

$$\begin{cases} M_i = \left[M_{i1}, \ldots, M_{im_i}\right] \in R_0^{1\times m_i} \\ R_i = \left[R_{i1}, \ldots, R_{im_i}\right] \in R_0^{m_i} \\ S_i = \left[S_{i1}, \ldots, S_{im_i}\right] \in R_0^{m_i} \end{cases} \tag{14}$$

In actual situations, $\hat{\rho}_i^h(t)$ is an estimate value of the unknown failure factor $\rho_i^h(t)$, and equation (15) shows that the adjustment with respect to the adaptive fault-tolerant control rate.

$$\frac{d\hat{\rho}_{if}^h(t)}{dt} = -\alpha_{if}\left[M_{if}R_{if} + M_{if}S_{if}\right], \quad f = 1, 2, \ldots, m_i \tag{15}$$

In equation (15), α_{if} is a constant greater than zero.

$\hat{\sigma}_{jik}^h(t)$ is the estimated value of the unknown failure factor $\sigma_{jik}^h(t)$, and equation (16) shows the adjustment of the adaptive fault-tolerant control rate.

$$\frac{d\hat{\sigma}_{jik}^h}{dt} = \beta_{jik} x_i^T(t) P_i a_{1S}^{ijk} a_{2T}^{jik} x_j(t), \quad k = 1, 2, \ldots, q_{ji} \tag{16}$$

In equation (16), β_{jik} is a constant greater than zero, a_{1S}^{ijk}, a_{1T}^{ijk} are the elements of the kth row of A_{1S}^{ij}, A_{2T}^{ji}, and $\hat{d}_i(t)$ is the estimated value of the external disturbance $d_i(t)$. Equation (17) shows the adjustment of the adaptive fault-tolerant control rate.

$$\frac{d\hat{d}_{ig}(t)}{dt} = \gamma_{ig} x_i^T(t) P_i b_{1d}^{ig}, \quad g = 1, 2, \ldots, p_i \tag{17}$$

In equation (17), γ_{ig} is a constant greater than zero and b_{1d}^{ig} is the gth column element of matrix B_{1d}^i.

For the closed-loop integrated fault-tolerant system described in equation (13), the control gain equation in the proposed distributed robust adaptive fault-tolerant state feedback controller is given by equation (18):

$$\hat{K}_1(t) = \left[\hat{K}_{11}(t), \ldots, \hat{K}_{1m_i}(t)\right]^T \in R^{m_i\times n_i} \tag{18}$$

Equation (18) is adjusted by the following adaptive fault-tolerant control rate in equation (19):

$$\frac{d\hat{K}_{1f}(t)}{dt} = -\omega_{1f} x_i x_i^T P_i b_{1u}^{if} \quad i = 1, 2, \ldots, N, \quad f = 1, 2, \ldots, m_i \tag{19}$$

In equation (19), ω_{1f} is a positive constant, b_{1u}^{if} is the fth column element of matrix B_{1u}^i, and $\hat{K}_2$ is a matrix with the appropriate dimension.

$$\hat{\boldsymbol{K}}_3(t) = \left[\hat{K}_{31}(t), \ldots, \hat{K}_{3m_i}(t)\right] \in \boldsymbol{R}^{m_i\times n_i} \tag{20}$$

Equation (20) is adjusted by the following adaptive fault-tolerant control rate in equation (21):

$$\frac{d\hat{\boldsymbol{K}}_{3k}(t)}{dt} = -\omega_{3k}\sum_{j=1}^{N} x_j x_i^T \boldsymbol{P}_i \boldsymbol{B}_{1u}^i \hat{\rho}_i^h k_{i2k} \hat{\sigma}_{jik}^h \tag{21}$$

In equation (21), ω_{3k} is any non-zero positive constant and k_{i2k} is the kth column element of matrix $\hat{K}_2$.

$$\hat{\boldsymbol{K}}_4(t) = \left[\hat{K}_{41}(t), \ldots, \hat{K}_{4m_i}(t)\right]^T \in \boldsymbol{R}^{m_i\times n_i} \tag{22}$$

Equation (22) is adjusted by the following adaptive fault-tolerant control rate in equation (23) as follows:

$$\frac{d\hat{\boldsymbol{K}}_{4g}(t)}{dt} = -\omega_{4g}\hat{d}_{ig} x_i^T \boldsymbol{P}_i \boldsymbol{B}_{1u}^i \hat{\rho}_i^h \tag{23}$$

In equation (23), ω_{4g} is a non-zero positive constant.

Equation (24) shows the error of the system:

$$\begin{cases} \Delta\rho_i^h(t) = \hat{\rho}_i^h(t) - \rho_i^h \\ \Delta\sigma_{ji}^h(t) = \hat{\sigma}_{ji}^h(t) - \sigma_{ji}^h \\ \Delta d_i(t) = \hat{d}_i(t) - d_i \\ \Delta K_1(t) = \hat{K}_1(t) - K_1 \\ \Delta K_3(t) = \hat{K}_3(t) - K_3 \\ \Delta K_4(t) = \hat{K}_4(t) - K_4 \end{cases} \tag{24}$$

In equation (24), since ρ_i^h, σ_{ji}^h, d_i, K_1, K_2, K_3 are unknown constants, equation (25) is as follows:

$$\begin{cases} \Delta\rho_i^h(t) = \hat{\rho}_i^h(t) \\ \Delta\sigma_{ji}^h(t) = \hat{\sigma}_{ji}^h(t) \\ \Delta d_i(t) = \hat{d}_i(t) \\ \Delta K_1(t) = \hat{K}_1(t) \\ \Delta K_3(t) = \hat{K}_3(t) \\ \Delta K_4(t) = \hat{K}_4(t) \end{cases} \tag{25}$$

Theorem 1: The closed-loop associative integrated system should satisfy the following assumptions:

Supposition 1: The matrix $\left\{\boldsymbol{A}_{1T}^i, \boldsymbol{B}_{1U}^i \rho_i^h\right\}$, $i = 1, 2, \ldots, N$ of the quadrotor UAV in the system is completely controllable in the failure mode of the wireless communication associated link failure mode [10].

Supposition 2: For all failure modes present in the system, there is a matrix K_{3ij} with appropriate dimensions such that $A_{1S}^{ij} = B_{1U}^i \hat{\rho}_i^h K_{3ij}$ and $\hat{\rho}_i^h$ is an adaptive estimate value of ρ_i^h.

Then, the following conclusion is correct: if there is a positive symmetric matrix $P_i > 0$, $\hat{\rho}_{if}^h(t)$, $\hat{\sigma}_{jik}^h(t)$, $\hat{d}_{ig}(t)$ and the system's state of control gain matrix $\hat{K}_1(t)$, $\hat{K}_2(t)$, $\hat{K}_3(t)$ use the adaptive fault-tolerant rate to adjust by the above equations: (15), (16), (17), (19), (21) and (23). This closed-loop fault-tolerant system satisfies the Lyapunov second stability criterion with any parameter such as $\rho_i^h \in \Delta\rho_i^h$ and $\sigma_{ji}^h \in \Delta\sigma_{ji}^h$; i.e., the system maintains asymptotic stability.

Certification: First, we define the Lyapunov function [10], equation (26), as follows for the aforementioned closed-loop fault-tolerant correlation system.

$$\begin{aligned} V(t) = &\sum_{i=1}^{N} x_i^T P_i x_i + \sum_{i=1}^{N}\sum_{f=1}^{m_i} \frac{\left(\Delta\rho_{if}^h\right)^2}{\alpha_{if}} \\ &+ \sum_{i=1}^{N}\sum_{j=1}^{N}\sum_{k=1}^{q_{ji}} \frac{\left(\Delta\sigma_{jik}^h\right)^2}{\beta_{jik}} + \sum_{i=1}^{N}\sum_{g=1}^{p_i} \frac{\Delta d_{ig}^2}{\gamma_{ig}} \\ &+ \sum_{i=1}^{N}\sum_{f=1}^{m_i} \rho_{if}^h \Delta K_{1f}^T \omega_{1f}^{-1} \Delta K_{1f} \\ &+ \sum_{i=1}^{N}\sum_{k=1}^{q_{ji}} \Delta K_{3f}^T \omega_{3k}^{-1} \Delta K_{3f} \\ &+ \sum_{i=1}^{N}\sum_{g=1}^{p_i} \Delta K_{4g}^T \omega_{4g}^{-1} \Delta K_{4g} \end{aligned} \tag{26}$$

In the system, there are two fault modes, $\rho_i^h \in \Delta\rho_i^h$ and $\sigma_{ji}^h \in \Delta\sigma_{ji}^h$, and the closed-loop system equation (13) shows that the derivative of the motion trajectory with respect to time t is given by equation (27):

$$\begin{aligned} \frac{dV(t)}{dt} = &\sum_{i=1}^{N} \left\{ x_i^T \left[\left(A_{1T}^i + B_{1u}^i \rho_i^h \hat{K}_1\right)^T P_i \right.\right. \\ &\left.\left. + P_i \left(A_{1T}^i + B_{1u}^i \rho_i^h \hat{K}_1\right) \right] x_i \right. \\ &+ 2x_i^T P_i \left[\sum_{j=1}^{N} \left(A_{1S}^{ij} \sigma_{ji}^h A_{2T}^{ji} + B_{1u}^i \rho_i^h K_2 \hat{\sigma}_{ji}^h \hat{K}_3 \right) x_j \right] \\ &+ 2x_i^T P_i B_{1d}^i d_i + 2x_i^T P_i B_{1u}^i \rho_i^h \hat{K}_4 \hat{d}_i \\ &+ \sum_{f=1}^{m} \frac{2\Delta\rho_{if}^h \cdot \frac{d\Delta\rho_{if}^h}{dt}}{\alpha_{if}} \\ &+ \sum_{j=1}^{N}\sum_{k=1}^{q_{ji}} \frac{2\Delta\sigma_{jik}^h \cdot \frac{d\Delta\sigma_{jik}^h}{dt}}{\beta_{jik}} \\ &+ \sum_{g=1}^{p_i} \frac{2\Delta d_{ig} \cdot \frac{d\Delta d_{ig}}{dt}}{\gamma_{ig}} \\ &+ \sum_{f=1}^{m} 2\rho_{if}^h \Delta K_{1f}^T \omega_{1f}^{-1} \frac{d\Delta K_{1f}}{dt} \\ &+ \sum_{j=1}^{N}\sum_{k=1}^{q_{ji}} 2\Delta K_{3k}^T \omega_{3k}^{-1} \frac{d\Delta K_{3f}}{dt} \\ &\left. + \sum_{g=1}^{p_i} 2\Delta K_{4g}^T \omega_{4g}^{-1} \frac{d\Delta K_{4g}}{dt} \right\} \end{aligned} \tag{27}$$

From the original formula, we can obtain equation (28) as follows:

$$\begin{aligned} &\frac{dV(t)}{dt} \\ &= \sum_{i=1}^{N} \left\{ x_i^T \left[\left(A_{1T}^i + B_{1u}^i \rho_i^h \hat{K}_1\right)^T P_i \right.\right. \\ &\quad \left.\left. + P_i \left(A_{1T}^i + B_{1u}^i \rho_i^h \hat{K}_1\right) \right] x_i \right. \\ &\quad + 2x_i^T P_i \cdot \sum_{j=1}^{N}\sum_{k=1}^{q_{ji}} a_{1S}^{ijk} \sigma_{jik}^h a_{2T}^{jik} x_j + \sum_{j=1}^{N}\sum_{k=1}^{q_{ji}} \frac{2\Delta\sigma_{jik}^h \cdot \frac{d\sigma_{jik}^h}{dt}}{\beta_{jik}} \\ &\quad + 2x_i^T P_i B_{1u}^i \rho_i^h \sum_{j=1}^{N}\sum_{k=1}^{q_{ji}} K_{2k} \hat{\sigma}_{jik}^h \hat{K}_{3k} x_j + 2x_i^T P_i \sum_{g=1}^{p_i} b_{1d}^{ig} d_{ig} \\ &\quad + 2x_i^T P_i B_{1u}^i \rho_i^h \sum_{g=1}^{p_i} \hat{K}_{4g} \hat{d}_{ig} + \sum_{f=1}^{m} \frac{2\Delta\rho_{if}^h \cdot \frac{d\Delta\rho_{if}^h}{dt}}{\alpha_{if}} \\ &\quad + \sum_{g=1}^{p_i} \frac{2\Delta d_{ig} \cdot \frac{d\Delta d_{ig}}{dt}}{\gamma_{ig}} + \sum_{f=1}^{m} 2\rho_{if}^h \Delta K_{1f}^T \omega_{1f}^{-1} \frac{d\Delta K_{1f}}{dt} \\ &\quad \left. + \sum_{j=1}^{N}\sum_{k=1}^{q_{ji}} 2\Delta K_{3k}^T \omega_{3k}^{-1} \frac{d\Delta K_{3f}}{dt} + \sum_{g=1}^{p_i} 2\Delta K_{4g}^T \omega_{4g}^{-1} \frac{d\Delta K_{4g}}{dt} \right\} \end{aligned} \tag{28}$$

Then, we select the previous adaptive fault-tolerant control rate [11]. We can adjust three parameters, $\hat{\rho}_i^h(t)$, $\hat{\sigma}_{jik}^h(t)$, $\hat{d}_{ig}(t)$, to ensure that there are two constants $K_{3k}, K_{4g} \in R^{n_i}$, $k = 1, 2, \ldots, q_{ji}$, $g = 1, 2, \ldots, p_i$, given by equations (29) and (30):

$$\begin{cases} \sum_{i=1}^{N}\sum_{j=1}^{N}\sum_{k=1}^{q_{ji}} 2x_i^T P_i B_{1u}^i \hat{\rho}_i^h K_{2k} \hat{\sigma}_{jik}^h K_{3k} x_j \\ \le -\sum_{i=1}^{N}\sum_{j=1}^{N}\sum_{k=1}^{q_{ji}} 2x_i^T P_i a_{1S}^{ijk} \hat{\sigma}_{jik}^h a_{2T}^{ijk} x_j \end{cases} \tag{29}$$

$$\sum_{i=1}^{N}\sum_{g=1}^{p_i} 2x_i^T P_i B_{1u}^i \hat{\rho}_i^h K_{4g} \hat{d}_{ig} \le -\sum_{i=1}^{N}\sum_{g=1}^{p_i} 2x_i^T P_i b_{1d}^{ig} \hat{d}_{ig} \tag{30}$$

Then, we can change the original equation (28) to equation (31) as follows:

$$\begin{aligned} &\frac{dV(t)}{dt} \\ &\le \sum_{i=1}^{N} \left\{ x_i^T \left[\left(A_{1T}^i + B_{1u}^i \rho_i^h \hat{K}_1\right)^T P_i \right.\right. \\ &\quad \left.\left. + P_i \left(A_{1T}^i + B_{1u}^i \rho_i^h \hat{K}_1\right) \right] x_i \right. \end{aligned}$$

$$+\sum_{j=1}^{N}\sum_{k=1}^{q_{ji}}2x_i^T P_i a_{1S}^{ijk}\hat{\sigma}_{jik}^h a_{2T}^{jik}x_j-\sum_{g=1}^{p_i}2x_i^T P_i b_{1d}^{ig}\hat{d}_{ig}$$
$$-\sum_{j=1}^{N}\sum_{k=1}^{q_{ji}}2x_i^T P_i B_{1u}^i\Delta\rho_i^h K_{2k}\hat{\sigma}_{jik}\hat{K}_{3k}x_j+\sum_{g=1}^{p_i}2x_i^T P_i b_{1d}^{ig}\hat{d}_{ig}$$
$$+\sum_{j=1}^{N}\sum_{k=1}^{q_{ji}}2x_i^T P_i\hat{\rho}_i^h K_{2k}\hat{\sigma}_{jik}^h\hat{K}_{3k}x_j+\sum_{f=1}^{m}\frac{2\Delta\rho_{if}^h\cdot\frac{d\Delta\rho_{if}^h}{dt}}{\alpha_{if}}$$
$$+\sum_{f=1}^{m}2\rho_{if}^h\Delta K_{1f}^T\omega_{1f}^{-1}\frac{d\Delta K_{1f}}{dt}+\sum_{j=1}^{N}\sum_{k=1}^{q_{ji}}2\Delta K_{3k}^T\omega_{3k}^{-1}\frac{d\Delta K_{3f}}{dt}$$
$$+\sum_{g=1}^{p_i}2\Delta K_{4g}^T\omega_{4g}^{-1}\frac{d\Delta K_{4g}}{dt}\Bigg\} \tag{31}$$

Then, we can obtain equation (32) as follows:

$$\frac{dV(t)}{dt}$$
$$\le\sum_{i=1}^{N}\Bigg\{x_i^T\left[\left(A_{1T}^i+B_{1u}^i\rho_i^h\hat{K}_1\right)^T P_i+P_i\left(A_{1T}^i+B_{1u}^i\rho_i^h\hat{K}_1\right)\right]x_i$$
$$+\sum_{j=1}^{N}\sum_{k=1}^{q_{ji}}2x_i^T P_i B_{1u}^i\hat{\rho}_i^h K_{2k}\hat{\sigma}_{jik}^h\hat{K}_{3k}x_j$$
$$+\sum_{g=1}^{p_i}2x_i^T P_i B_{1u}^i\hat{\rho}_i^h\Delta K_{4g}\hat{d}_{ig}$$
$$-\sum_{j=1}^{N}\sum_{k=1}^{q_{ji}}2x_i^T P_i B_{1u}^i\Delta\rho_i^h K_{2k}\hat{\sigma}_{jik}^h\hat{K}_{3k}x_j$$
$$-\sum_{g=1}^{p_i}2x_i^T P_i B_{1u}^i\Delta\rho_i^h\hat{K}_{4g}\hat{d}_{ig}+\sum_{f=1}^{m}\frac{2\Delta\rho_{if}^h\cdot\frac{d\Delta\rho_{if}^h}{dt}}{\alpha_{if}}$$
$$+\sum_{f=1}^{m}2\rho_{if}^h\Delta K_{1f}^T\omega_{1f}^{-1}\frac{d\Delta K_{1f}}{dt}+\sum_{j=1}^{N}\sum_{k=1}^{q_{ji}}2\Delta K_{3k}^T\omega_{3k}^{-1}\frac{d\Delta K_{3f}}{dt}$$
$$+\sum_{g=1}^{p_i}2\Delta K_{4g}^T\omega_{4g}^{-1}\frac{d\Delta K_{4g}}{dt}\Bigg\} \tag{32}$$

For Supposition 2, we can obtain that when $\rho_i\in\Delta\rho_{ij}^h$ [12], [13], $P_i>0$ and K_1 will be satisfied as in equation (33):

$$\left[\left(A_{1T}^i+B_{1u}^i\rho_i^h\hat{K}_1\right)^T P_i+P_i\left(A_{1T}^i+B_{1u}^i\rho_i^h\hat{K}_1\right)\right]<0 \tag{33}$$

Then, we can obtain equation (32) in the same way as equation (34):

$$\frac{dV(t)}{dt}\le\sum_{i=1}^{N}\Bigg\{x_i^T\left[\left(A_{1T}^i+B_{1u}^i\rho_i^h\hat{K}_1\right)^T P_i+P_i\left(A_{1T}^i+B_{1u}^i\rho_i^h\hat{K}_1\right)\right]x_i$$
$$+2x_i^T PB_{1u}^i\rho_i^h\hat{K}_1x$$
$$+\sum_{f=1}^{m}2\Delta K_1^T\omega_{1f}^{-1}\frac{d\Delta K_{1f}}{dt}$$
$$+2\sum_{f=1}^{m_i}\Delta\rho_{if}^h M_{if}R_{if}+2\sum_{f=1}^{m_i}\Delta\rho_{if}^h M_{if}S_{if}$$
$$+\sum_{f=1}^{m_i}2\frac{\Delta\rho_{if}^h\frac{d\Delta\rho_{if}^h}{dt}}{\alpha_{if}}\Bigg\} \tag{34}$$

We make the following definition:

$$Q_i=-\left[\left(A_{1T}^i+B_{1u}^i\rho_i^h\hat{K}_1\right)^T P_i+P_i\left(A_{1T}^i+B_{1u}^i\rho_i^h\hat{K}_1\right)\right]>0 \tag{35}$$

We select the adaptive fault-tolerant control rate [14], [15] that has already been defined in equations (15) and (19). Then, the improved version of equation (34) can be written as follows:

$$\frac{dV(t)}{dt}\le-\sum_{i=1}^{N}x_i^T Q_i x_i \tag{36}$$

In equation (36), we find that when the parameter x only satisfies $x\neq0$, dV (t)/dt <0; thus, the system state variable $x(t)$ asymptotically converges to 0, and then all signals are bounded. That is, the system satisfies the Lyapunov second stability criterion, and the system remains asymptotically stable.

The proof is complete.

V. SIMULATION ANALYSIS

To verify the performance index and anti-interference performance of the hierarchical distributed robust adaptive fault-tolerant controller with a real-time wireless network system, a simulation test is carried out in the TrueTime2.0 environment in MATLAB/SIMULINK. The initial state parameters of the system are as follows:

The initial state of the system is as follows:

$$x(0)=\begin{bmatrix}0&0&0&0&0&0\end{bmatrix}^T;$$

The robust adaptive fault tolerance initial value is : $\hat{k}_3(t)=1.9702$.

The type of wireless network is selected as: 802.15.4; The wireless network data transmission rate is: $0<W_{DR}\le21125$bit/s, $W_{DR}>21125$bit/s.

The critical data transmission rate corresponding to the switching system is 21125bit/s.

The minimum data frame length is 100bit/s.

The system's packet loss rate is $0.465\in[0,1]$.

The calculation time of the system's sensors, controllers and actuators is 0.4 ms.

The wireless network delay time is 35 ms.

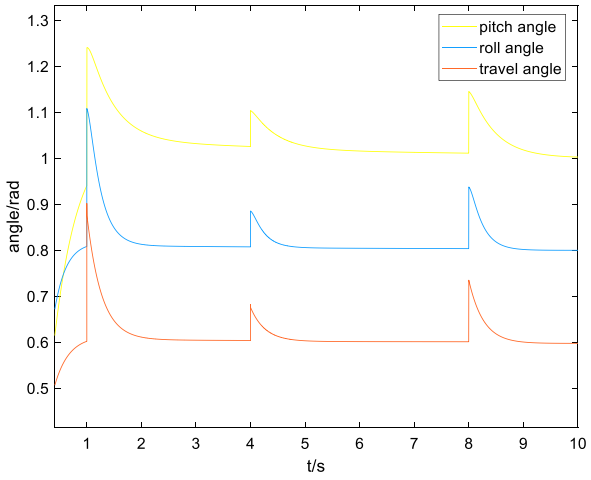

FIGURE 2. Angle curve.

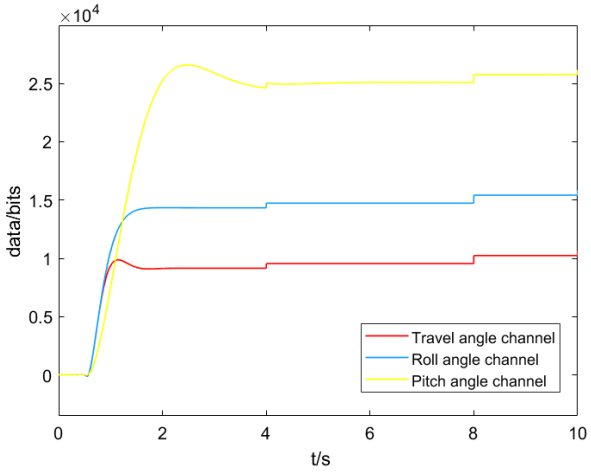

FIGURE 3. Variation in the three-angle channel data volume.

The tunable control parameters are:

$$\begin{cases} v(t) = 2.592 + e^{-0.0251t} \\ h(t) = e^{-10.241t} \\ \partial_{if} = 100 \\ \rho_{ji}^{h} = \sigma_{ji}^{h} = 0.1 \\ \bar{\rho}_{ji}^{h} = \bar{\sigma}_{ji}^{h} = 0.9. \end{cases} \tag{37}$$

It is assumed that the flight system of the drone is subjected to external disturbances such as strong winds in the first 2 seconds and is abstracted into a step signal with an amplitude of 0.1. When the external disturbances come to an end, the second disturbance is followed by physical damage in the 4th second, causing an interrupt and drift fault of an actuator of the power patrol quadrotor UAV system and drifting to $0.81 + 0.81e^{-t}$. In the last 8 seconds, the wireless communication module of the flight system of the human machine has a communication transmission delay and a packet loss failure, and the failure continues until the end. The simulation diagram is shown in Figure 2-8.

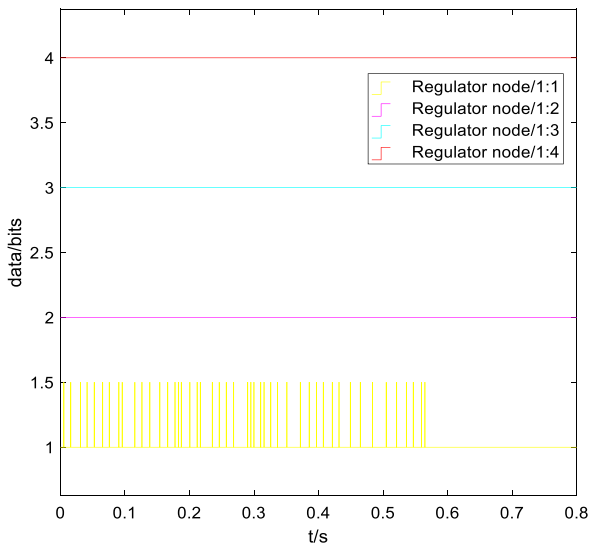

FIGURE 4. Variation in the wireless network executor node packet acceptance.

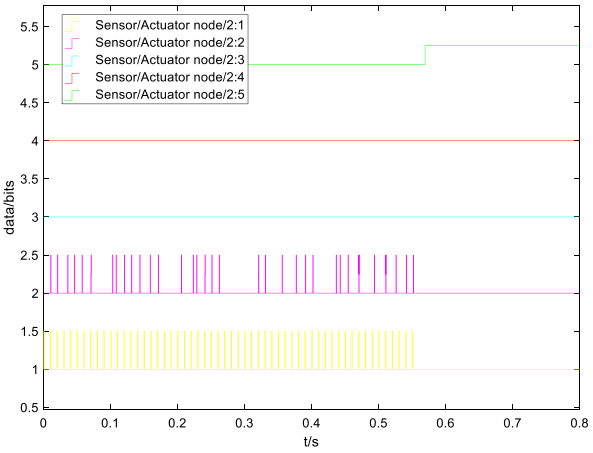

FIGURE 5. Variation in the wireless network regulator node data packet acceptance.

It can be seen from Figure 2 that before the initial operation at 2 seconds, when a step signal with a magnitude of 0.1 is added to the system as external interference, the system will be in the initial state of the distributed robust adaptive fault-tolerant controller $u_i(t)$. The control is continuously adjusted to approximate the desired reference value. After a short dynamic adjustment, the pitch angle, roll angle and travel angle can accurately track the expected reference value of the system. The specific realization of the whole system is as follows: at 4 seconds, an actuator of the drone has an interruption fault, and the drift of the drone as a whole has occurred. It can be seen from the figure that at 2 seconds, the curve exhibits peaks of 0.697, 1.112, and 1.245, which correspond to the original values of 0.6, 0.8, and 1.0, and the fluctuation errors are +0.097, +0.312, and +0.245, respectively. At 4 seconds, 8 seconds and 10 seconds, the curve exhibits two peaks from the original values of 0.6,

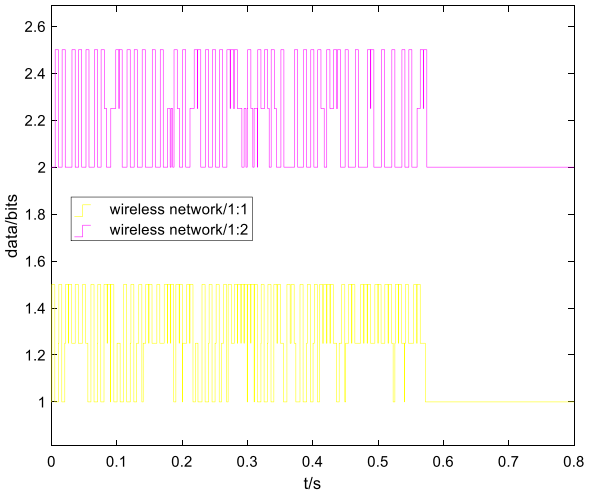

FIGURE 6. Wireless network node data packet transmission diagram.

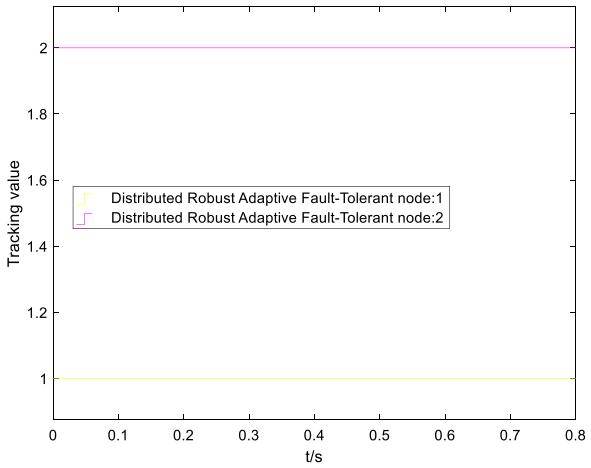

FIGURE 7. Distributed robust adaptive fault-tolerant node tracking value change graph.

0.8, and 1.0, with one normal peak and one shifted peak, and the peak values are 0.651, 0.874, 1.097, 0.712, 0.954, 1.058. The fluctuation errors are +0.051, +0.074, +0.097, +0.112, +0.154, and +0.058, and the error is within the allowable range. In the whole simulation process we also find that the overshoot of pitch angle, roll angle and travel angle is between 8% and 15%. From a theoretical point of view, the system is unstable, the main reason is that the designed controller focuses on external disturbances, actuator failures and associated link failures. The stability of the system is only guaranteed to be asymptotically stable. That is, the pitch angle, roll angle and yaw angle can be asymptotically stable with the adaptive fault tolerance of the designed controller, thus indicating that the designed controller performs well.

Before the initial operation at 2 seconds, with the start of the quadrotor UAV, the drone's three-angle channels for the pitch, roll and yaw during the anti-interference process slowly reach a stable value. In the 8th second, it is assumed

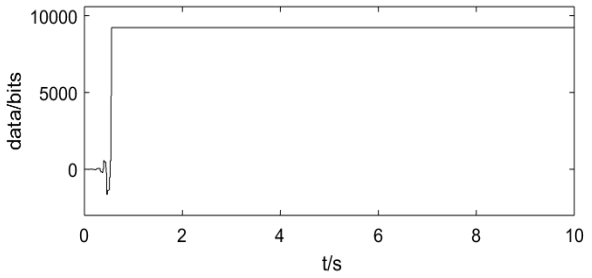

FIGURE 8. System state feedback response curve.

that the UAV airborne wireless communication transmission module has a packet loss delay communication failure. It can be seen from the figure that the system has packet loss and a delayed communication failure in the 8th second, the three channels of data exhibit a jump of nearly 1000 bits of data, and then the data volume of the three channels returns to a normal value, as shown in Figure 2, because the elevation angle, roll angle and yaw angle in Figure 2 act against the malfunction of the actuator. After reaching a steady state, the amount of data after the new transition is also stable. That is, the three data channels of pitch, roll and yaw can ensure that the overall wireless communication quadrotor UAV flight system is asymptotically stable with the adaptive fault tolerance of the designed controller. This shows that the designed controller performs well.

Figures 4-7 show the node packet transmission and acceptance of the wireless network actuator and regulator and distributed robust adaptive fault-tolerant node tracking value.

It can be seen from Figure 8 that, with the designed controller, the data transmission of the quadrotor UAV wireless communication real-time flight system is asymptotically stable with a packet loss rate of 46.5% and a network delay of 35 ms. This result verifies the effectiveness of the designed controller.

VI. CONCLUSION

In this paper, a quadrotor UAV is considered as a research object and a corresponding mathematical model is established. We design a distributed robust adaptive fault-tolerant controller for a real-time wireless network quadrotor UAV flight system that combines a next-generation wireless network and a quadrotor UAV, where the control algorithm is based on robust adaptive fault-tolerant control theory. We perform a fault-tolerant test simulation in which the system experiences information communication faults, such as packet loss failure, random delay failure, and actuator faults, which include interruption failure and drift failure. As shown above, the simulation results show that the aircraft can gradually recover to a stable state in the presence of wireless communication failure and actuator failure. During operation, we can achieve good control performance and accuracy, and the three angle channels of pitch angle, roll angle and travel angle can maintain stable values. The wireless information communication transmission capability of the UAV is improved.

Overall, the system presents relatively good distributed fault tolerance performance. The simulation results verify that the designed distributed robust fault-tolerant controller exhibits asymptotic stability and provides a theoretical basis for the subsequent construction of a small ground-to-air wireless ad hoc network.

REFERENCES

[1] Y. Qinghua, S. Zhaoqing, and S. Lei, "Four-rotor air-craft modeling, control and simulation," *J. Nav. Aeronaut. Eng. College*, vol. 5, pp. 499–502, 2009.
[2] W. Zhifang, F. Xingjian, and L. Tong, "LQR optimization control of four-rotor craft," *Sensor World*, vol. 3, pp. 17–23, 2017.
[3] W. Zhifang, F. Xingjian, S. Jie, and Y. Jianguo, "Robust adaptive fault tolerate controlfor stability control of electric patrol survey UAV," *Eng. J. Wuhan Univ.*, vol. 7, pp. 646–653, 2018.
[4] Z. Wang, J. Shen, X. Fu, and B. Chen, "Robust adaptive optimization algorithm for stability control of electric patrol survey UAV," in *Proc. Int. Conf. Comput. Intell. Inf. Syst. (CIIS)*, vol. 1, Apr. 2017, pp. 108–115.
[5] Y. Xinzhe, "Observer-based active fault-tolerant control of four-rotor helicopter attitude system," Nanjing Univ. Aeronaut., Nanjing, China, Tech. Rep., 2012.
[6] Z. Yong, "Design and implementation of fault-tolerant control system for four-rotor craft," Univ. Electron. Sci. Technol., Chengdu, China, Tech. Rep., 2013.
[7] L. Feifei, "Research on adaptive fault-tolerant control algorithm for four-rotor helicopter attitude control system," Nanjing Univ. Aeronaut., Nanjing, China, Tech. Rep., 2012.
[8] J. Xiaozheng, Y. Zhonghu, and L. Yanping, *Active Fault-Tolerant Control Theory Adaptive Method*. Beijing, China: Electronic Industry Press, 2014.
[9] Z. Dengfeng, W. Zhiquan, and H. Xiaodong, *Satisfaction Fault Tolerance Control*, vol. 3. Beijing, China: Science Press, 2014.
[10] J. Xiaozheng, Y. Guanghong, C. Xiaohuan, and C. Weiwei, "Fault-tolerant control system robust H_∞ and adaptive compensation design," *J. Autom.*, vol. 39, no. 1, pp. 31–42, 2013.
[11] H. Shousong, *Automatic Control Principle*. Beijing, China: Science Press, 2013.
[12] H. X. Yang, X. X. Yang, and W. H. Zhang, "Distributed control of spacecraft formation using improved cyclic pursuit with beacon guidance," *Appl. Mech. Mater.*, vols. 138–139, pp. 38–42, Nov. 2011.
[13] A. Khosravian and M. Namvar, "Rigid body attitude control using a single vector measurement and gyro," *IEEE Trans. Autom. Control*, vol. 57, no. 5, pp. 1273–1279, May 2012.
[14] Z. W. A. Yuli, *Networked Control System Analysis and Design*. Beijing, China: Science Press, 2012.
[15] X. Ye, S. Liu, and P. X. Liu, "Modelling and stabilisation of networked control system with packet loss and time-varying delays," *IET Control Theory Appl.*, vol. 4, no. 6, pp. 1094–1100, 2010.
[16] F. Yang, W. Wang, Y. Niu, and Y. Li, "Observer-based H_∞ control for networked systems with consecutive packet delays and losses," *Int. J. Control Automat. Syst.*, vol. 8, no. 4, pp. 769–775, 2010.

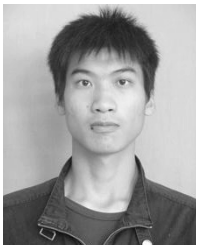

ZHIFANG WANG received the B.S. degree in automation from the Jilin Institute of Chemical Technology, Jilin, in 2015, and the M.S degree in control theory and control engineering from the Beijing University of Science and Technology Information, Beijing, in 2018, respectively. He is currently pursuing the Ph.D. degree in electronics and communication engineering with the Beijing University of Posts and Telecommunications (BUPT), Beijing. His research interests include networked robust fault tolerant control for wireless communication systems, and amorphous ad hoc network design.

JIANGUO YU received the Ph.D. degree in electromagnetic field and microwave technology from the Beijing University of Posts and Telecommunications (BUPT), Beijing, in 1997. After graduation, he worked for 15 years with the Fiberhome Technology Group. He has served as an Engineer, a Senior Engineer, and a Professor-Level Senior Engineer. He served as the Deputy Head for the overall group of major cross-themes of the Opto-electronics, Communication, and Computer Networks, and a full-time overall group member. He designed and established the World's first multi-vendor equipment interconnection and mutual interoperability, operation, unified high-speed information optical network for network management. He is currently a Professor with the Beijing University of Posts and Telecommunications and the Ph.D. Tutor. He is responsible for completing the 3G/4G base station, fiber remote base station, digital fiber optic repeater, 3G/4G signal source, the development and conversion of the frequency sweeper and winning the bid for China Telecom, China Mobile, and China Unicom. He was elected to the National 863 Expert Group, in April 1999. His current research interests include microwave, millimeter wave, terahertz wave, and light wave.

SHANGJING LIN (S'11) received the B.E. degree in electronics information engineering from the Communication Command College, Wuhan, China, in 2008, the M.E. degree in communication engineering from the Wuhan Institution of Posts and Telecommunications, Wuhan, China, in 2011, and the Ph.D. degree from the Beijing University of Posts and Telecommunications, Beijing, China, in 2016. She was a Visiting Ph.D. Student with CSIRO, Australia, from 2014 to 2015. She currently holds a Postdoctoral position with the Beijing University of Posts and Telecommunications. Her research interests include radio resource management, mobile social networks, and game theory. She was a recipient of the Rohde and Schwarz Scholarship.

JUNGUO DONG received the B.S. degree in opto-electronic information science and engineering from the Beijing University of Posts and Telecommunications (BUPT), Beijing, China, in 2017, where he is currently pursuing the M.S. degree in electronic science and technology. His research interests include wireless communication, network platform construction, and network simulation.

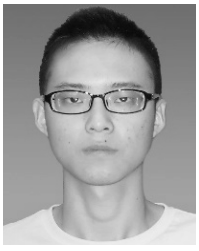

ZHEN YU received the B.S. degree in communication engineering from Northeastern University (NEU), Shenyang, Liaoning, in 2017. He is currently pursuing the M.S. degree in electronics and communication engineering with the Beijing University of Posts and Telecommunications (BUPT), Beijing. His research interests include wireless communication, routing protocol, and location algorithm design.